Proceedings of the Combustion Institute, Volume 29, 2002/pp. 1565–1572

CHARACTERISTICS OF LIFTED TRIPLE FLAMES STABILIZED IN THE NEAR FIELD OF A PARTIALLY PREMIXED AXISYMMETRIC JET

XIAO QIN, ISHWAR K. PURI AND SURESH K. AGGARWAL
University of Illinois at Chicago
Department of Mechanical Engineering (M/C 251)
842 W. Taylor St.
Chicago, IL 60607-7022, USA

The characteristics of lifted laminar triple flames in the near field of the burner exit are experimentally and numerically investigated. The flames are established by introducing a nitrogen-diluted rich mixture of methane and air from an inner tube and a lean mixture from a concentric outer tube. The temperature and major species concentrations are measured using thermocouples and gas chromatography, respectively. The flame liftoff heights are determined from C_2* chemiluminescence emission images recorded by an intensified CCD camera. A time-dependent, implicit numerical model that uses a detailed description of the chemistry and includes buoyancy effects is used to simulate the flame structures. The numerical results are validated through detailed comparisons with experimental measurements. Both the measured and simulated reaction zone topographies show that there is a similitude between the burner-stabilized and lifted flames. It is found that, unlike the highly nonlinear behavior of lifted flames in the far field of a jet, the liftoff height of near-field lifted flames exhibits a linear relationship with respect to the inner-flow velocity. Two kinds of oscillations, one induced by the instability in the inner flow and the other through buoyancy effects, have been observed. The former has a frequency of about 16 Hz and the latter of 4 Hz. After lifting, an unsteady triple flame moves downstream along the stoichiometric mixture fraction contour, and the axial velocity reaches a minimum value near the triple point. This velocity is close to the laminar burning velocity of unstretched stoichiometric methane-air flames. The hydrodynamic stretch increases with the increase in liftoff height and the curvature stretch decreases. There is a good correlation between the stretch rate, Lewis number, and flame propagation speed in both the rich and lean premixed zones of the lifted triple flame.

Introduction

The behavior of triple flames has been extensively studied because of their role in flame stabilization, flame spread, and re-ignition in turbulent combustion [1]. Lifted flames in laminar jets can provide a basic understanding of turbulent flame stabilization; these lifted flames often exhibit a triple flame structure at their base [2–5]. Chung and Lee [2,3] showed that for non-premixed laminar jets, propane and *n*-butane flames can be lifted while methane and ethane flames blow out directly from a burner-stabilized mode. Their analysis demonstrated that the Schmidt number (*Sc*) plays an important role in flame liftoff, and stable lifted flames are possible only for fuels for which $Sc > 1$ or less than 0.5. Kioni et al. [4] established lifted triple flames using nitrogen-diluted methane fuel and investigated the effect of strain rate. Ghosal and Vervisch [5] recently extended Chung and Lee's work and demonstrated analytically that a lifted laminar flame is possible for a fuel for which *Sc* is greater than a critical value Sc_{cr}, where Sc_{cr} can be less than unity. For values of $Sc < Sc_{cr}$ they showed that a lifted flame is subcritical and can only survive in a narrow parametric region.

Liñán [6] showed that there are two possibilities for the stabilization of non-premixed flames in laminar mixing layers: the flame can be either stabilized near a splitter plate, or it can be stabilized farther downstream in the form of a lifted flame. The liftoff height for typical laminar jet flames is usually on the order of 1–10 cm, and exhibits a highly nonlinear behavior with jet velocity and nozzle diameter. The lifted triple flames in the cited references are all stabilized in the far field of a jet flow. The behavior of lifted flames near the burner exit is different from that in the far field and is often associated with flame stabilization. Takahashi et al. [7] investigated the stabilization mechanism of non-premixed laminar flames, and reported no triple flame structure at the base of lifted flames. Instead, they proposed that a reaction kernel of high reactivity provides the radical flux and serves as a stabilization point that is located in a small premixing zone. A quantitative comparison was not possible because of the lack of experimental data.

Our objective is to examine the behavior of lifted triple flames near the burner exit for an axisymmetric jet flow and provide further insight into the

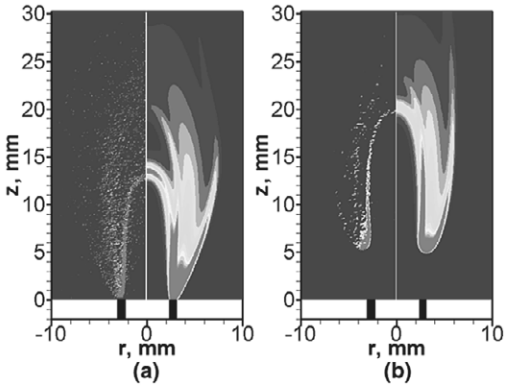

FIG. 1. Comparison between the experimentally obtained C_2* chemiluminescence intensities (left) and the predicted heat release rate contours (right) for attached (a) and lifted triple flames (b). The chemiluminescence image has been modified by multiplying each pixel intensity by a constant value defined by the ratio of the maximum specific heat release rate to the maximum pixel intensity.

stabilization and liftoff mechanisms. We have established lifted laminar triple flames at relatively low jet velocities by introducing a nitrogen-diluted rich methane-air mixture from an inner tube and a lean mixture from a concentric outer tube. A time-dependent, implicit numerical model with a detailed reaction mechanism is used to simulate the phenomena. The numerical results are validated through comparisons with experimental measurements and are used to investigate the effects of flame stretch, curvature, and flow dilatation on the stabilization of lifted triple flames.

Experimental and Numerical Methods

Atmospheric, partially premixed methane-air flames were established using an annular concentric burner that consists of a central tube with an inner diameter of 4.5 mm and an outer diameter of 6.1 mm, surrounded by a concentric tube with a diameter of 11.4 mm. The burner is made of brass and has a length of 200 mm to ensure fully developed Poiseuille flow at the exit. An acrylic cylinder with a diameter of 120 mm was placed concentrically around the burner to minimize the effect of outside disturbances. Methane-air fuel-rich mixtures and fuel-lean mixtures were introduced from the inner and outer tubes, respectively.

The excited C_2* free radical species is considered to be a good indicator of the reaction zone, and its light intensity varies linearly with the volumetric heat release [8]. The C_2* chemiluminescence images were obtained using an intensified CCD camera. The temperature measurements used uncoated 50-μm diameter R-type wire thermocouples with a junction-bead diameter of 140 $\pm$ 30 μm and were corrected for radiation heat losses. Thermocouple measurements have an absolute uncertainty of 70 K. Major species concentrations, namely, CH_4, O_2, CO_2, and CO, were measured using gas chromatography. The species were sampled at various locations using a narrow-tipped quartz microprobe of inlet diameter of 0.2 mm at the end and an orifice diameter of 100 μm. The sampling and analysis are described in detail elsewhere [9]. The relative uncertainties involved in the measurements lie between 5% and 10%.

The computational model is based on the algorithm developed by Katta et al. [10]. The simulation method is described in detail elsewhere [11]. The methane-air chemistry is modeled using a detailed mechanism that considers 24 species and 81 elementary reactions [12]. The mechanism has been validated for the computation of premixed flame speeds and for the structure of non-premixed and partially premixed flames [13]. The outflow boundaries in both directions are located sufficiently far from the respective inflow and symmetric boundaries so that the propagation of boundary-induced disturbances is minimized. Fully developed pipe flow in the inner tube and boundary layer velocity profiles outside the inner tube were used for the inflow boundary conditions. The computational domain of 100 $\times$ 50 mm in the axial (z) and radial (r) directions was represented by a staggered non-uniform 191 $\times$ 81 grid system.

Results and Discussion

Triple Flame Structures

Triple flames were established by introducing methane-air premixed mixtures at equivalence ratio ϕ_{in} = 2.5 through the inner tube, and by introducing a fuel-lean mixture ϕ_{out} = 0.35 through the outer tube. The inner tube exit velocities V_{in} were varied in the range of 0.20–1.23 m/s, while the outer tube velocity V_{out} was kept constant at 0.50 m/s. To lift the burner-stabilized flames at a relatively low Reynolds number, the inner fuel-rich mixture was diluted by nitrogen at 25% by volume. Flames without any dilution directly blew out from burner rim before liftoff as the flow velocity of the inner and outer flows was parametrically increased. This is in accord with Chung and Lee's results [2], that is, that pure methane cannot be used to establish stable lifted flames since its *Sc* has a value lower than unity but greater than 0.5. However, liftoff became possible by adding nitrogen to the inner fuel-rich mixture. Through gradual variation of V_{in} the flames could be lifted by 5.5 mm.

Figure 1 presents a comparison of the experimentally obtained C_2* chemiluminescence intensities

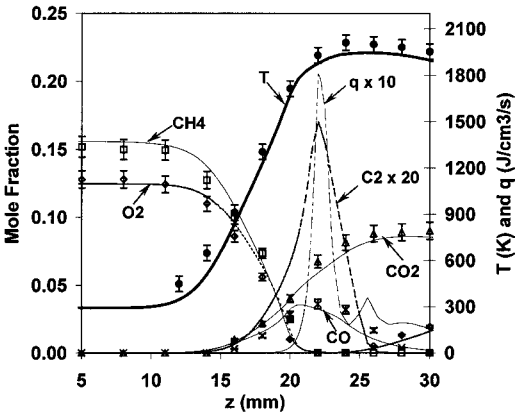

FIG. 2. Profiles of measured (symbols) and predicted (lines) temperatures, and of major species (CH_4, O_2, CO_2, CO species) concentrations along the centerline for a lifted flame. The predicted heat release rate (q) and sum of C2 species mole fraction are also plotted. The flame was established for the conditions: V_{in} = 0.6 m/s, V_{out} = 0.5 m/s, ϕ_{in} = 2.5, ϕ_{out} = 0.35.

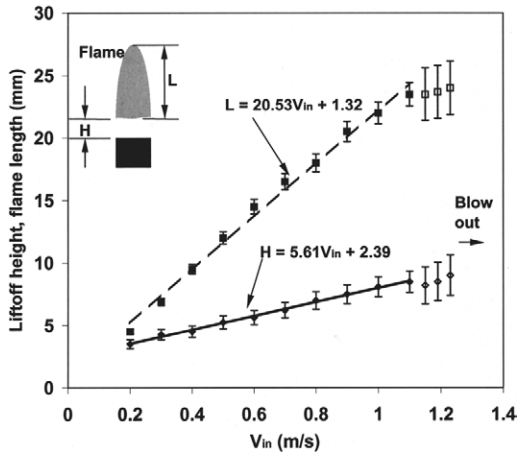

FIG. 3. Liftoff height (H) and flame length (L) with respect to inner-flow velocity for lifted triple flames. The flames were established for the conditions: V_{out} = 0.5 m/s, ϕ_{in} = 2.5, ϕ_{out} = 0.35 with varying inner-flow velocity. The open symbols represent the data corresponding to the second kind of oscillation.

(left) with the predicted heat release rate contours (right) for attached and lifted triple flames. The images clearly exhibit a triple flame structure for both the attached and lifted flames, with a non-premixed reaction zone located between a rich premixed and a lean premixed reaction zones. All three zones merge at the flame base. Because of nitrogen dilution, the lifted flames exhibit lower chemiluminescence intensity than their burner-stabilized undiluted counterparts. However, the two flames are similar with respect to overall topology, that is, the flame shapes, locations, and overall flame heights. While the predicted inner flame heights and the locations of the rich premixed and non-premixed reaction zones are in good agreement with the spatial profile of the measured C_2* intensity, the predicted lean premixed reaction zone has a much higher intensity than that shown by the measurement. The predicted liftoff height is in excellent agreement with the measurement. However, the predicted flame base is somewhat thicker and more rounded than the measurements, and we ascribe this to the low signal-to-noise ratio in the experiment. The lifted flame base is slightly inclined toward the axial centerline coordinate, and this has an effect on flame stabilization that is discussed later.

To validate the numerical model, the measured and predicted temperature and major species (CH_4, O_2, CO_2, and CO) concentrations for the lifted flames are compared along the centerline in Fig. 2. The predicted heat release rate (q) and C2 species mole fraction are also plotted to demonstrate the flame structure. The thermocouple temperatures in the region upstream of the flame are higher than in the prediction, which may be due to the conduction heat transfer along the thermocouple wire. The measured maximum temperature is slightly higher (2010 versus 1945 K) than the predicted value. Within the bounds of computational and experimental errors, the measured and predicted temperature and concentration profiles of the major species are in good agreement. Therefore, we conclude that the validated numerical model can be used to provide detailed insight into the triple flame structure. The CH_4 and O_2 mole fractions decrease rapidly in the preheat zone (in the region from 15 to 20 mm along the centerline). The CO concentration peaks in the inner premixed reaction zone, and is gradually depleted downstream as it is transported and consumed in the non-premixed reaction zone. The CO_2 concentration shows a peak in the highest temperature region, which is located downstream of the inner premixed reaction zone. Comparing Fig. 2 with Fig. 1b, it is apparent that the flame height determined using the heat release rate as a marker differs from that inferred through the maximum temperature isocontour.

Characteristics of Lifted Triple Flames

Figure 3 presents the experimental results showing the effect of inner-flow velocity on the liftoff height and flame length for the lifted triple flame. The flame length, which is defined as the height of the inner premixed reaction cone, increases linearly with V_{in}. Unlike the previously reported nonlinear behavior for lifted flames stabilized in the far field of a jet [2], the liftoff height of the triple flame considered herein increases linearly with V_{in} in the

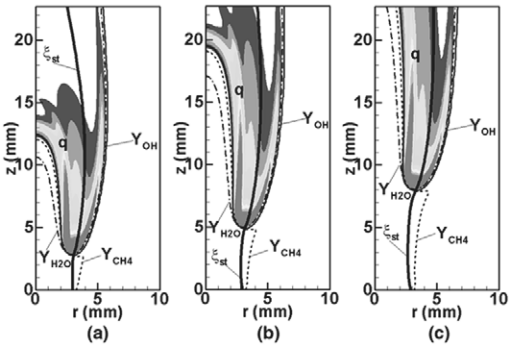

FIG. 4. Simulated CH_4, H_2O, and OH mass fraction isocontours and heat release rate (that begins at 50 J/(cm^3 s) with a 100 J/(cm^3 s) interval) for three cases: (a) T1, V_{in} = 0.4 m/s; (b) T2, V_{in} = 0.6 m/s, and (c) T3, V_{in} = 0.8 m/s. The thick solid line represents the stoichiometric mixture fraction ξ_{st} = 0.383. The flames were established for the conditions: V_{out} = 0.5 m/s, ϕ_{in} = 2.5, ϕ_{out} = 0.35. Y represents mass fraction.

range 0.2–1.1 m/s. For $V_{in} > 1.1$ m/s, the flame becomes unstable and oscillates, with blowout occurring occasionally after some periodic displacements. For $V_{in} > 1.23$ m/s, the flame directly blows out.

The lifted triple flames are very sensitive to disturbances in either the inner or outer flows. Two kinds of oscillations are observed using a high-speed video camera (Kodak EktaPro) in the velocity ranges from 0.6 to 1.1 m/s and 1.1 to 1.23 m/s, respectively. The former velocities have a uniform frequency of roughly 16 Hz despite their different inner-flow velocities, and the corresponding flames are relatively stable at their base. These disturbances oscillate with a maximum amplitude of ≈0.5 mm at the base and ≈1 mm at their tip, and are assumed to occur because of flow instabilities. The other oscillations have a lower frequency of ≈4 Hz, but larger amplitude. These are dominated by buoyancy effects and have been reported by Won et al. [14] for highly diluted propane flames in the developing region from the burner exit.

For the undiluted methane-air mixture of ϕ_{in} = 2.5, the Schmidt number (*Sc*) lies in the range 0.64–0.78 (with a mean value of 0.71), while for flames diluted with 25% N_2, *Sc* has values in the range 0.72–0.82 (with a mean value of 0.77). For methane, $Sc_{cr} \approx 0.8$ [5] so that these values are still subcritical. Flames with higher N_2 dilution have larger *Sc* values (e.g., for the flame diluted with 50% N_2 by volume, $Sc \approx 0.91$) and can be lifted up to 5 cm.

Parameters Characterizing Lifted Triple Flames

We now focus on the structure of lifted triple flames, emphasizing the effects arising because of flame stretch that characterize the flow field on the flame-displacement speed. Three flames with different inner-flow velocities, respectively, 0.4, 0.6, and 0.8 m/s (corresponding to cases T1, T2, and T3), are discussed. The outer-flow velocity for these flames is 0.5 m/s.

The mixture fraction ξ is defined as a linear combination of the elemental mass fractions on the basis of the formula suggested by Bilger [15], namely,

$$\xi = \frac{2Z_C/W_C + \frac{1}{2}Z_H/W_H + (Z_{O,2} - Z_O)/W_O}{2Z_{C,1}/W_C + \frac{1}{2}Z_{O,2}/W_O} \quad (1)$$

where Z_i denotes the mass fraction of the element i of atomic mass W_i, the subscripts C, H, and O refer to carbon, hydrogen, and oxygen, and the subscripts 1 and 2 refer to the fuel and oxidant reference states. The stoichiometric value, ξ_{st}, obtained by applying this definition provides a value of 0.383 for all three cases.

To define the flame surface, we need to select a transported scalar φ. There is some latitude regarding the choice of the scalar property. Najm and Wyckoff [16] used a particular value of the fuel mass fraction to identify the flame surface. Im and Chen [17] used a mass fraction contour of a product species (water) to describe the reaction zone of partially premixed H_2-air mixtures. Fig. 4 presents the CH_4, H_2O, and OH mass fraction contours, ξ_{st}, and heat release rate isocontours for cases T1 to T3. The H_2O isocontour represents the lean premixed reaction zone accurately, but not the inner rich premixed zone. The CH_4 isocontour is able to represent the rich premixed reaction zone accurately, but it decreases rapidly downstream of the triple point and fails to represent the lean premixed reaction zone. The OH isocontour clearly identifies the rich and lean premixed reaction zones, and, therefore, we will use it as a reaction zone marker. We find that an OH mass fraction of 2.0×10^{-5} traces the flame surface for all the cases considered. The triple point at the flame base is defined as the location of the intersection of ξ_{st} line and the significant OH isocontour.

The displacement speed of a flame S_d is defined as the normal component of the flame front speed relative to the local fluid velocity, that is [18],

$$S_d = -\frac{1}{\rho|\nabla\varphi|}[\nabla \cdot (\Gamma_\varphi \nabla\varphi) + \omega_\varphi] \quad (2)$$

where ρ denotes the density, Γ_φ denotes the diffusion coefficient for φ, and ω_φ is the volumetric rate of generation or destruction of φ. Following Chung and Law [19], the flame stretch, κ, is expressed as

$$\kappa = \nabla \cdot V_{fluid,t} + (V_{flame} \cdot \hat{n})(\nabla \cdot \hat{n}) \quad (3)$$

where V_{fluid} denotes the flow velocity at the flame surface, V_{flame} is the flame velocity in the inertial

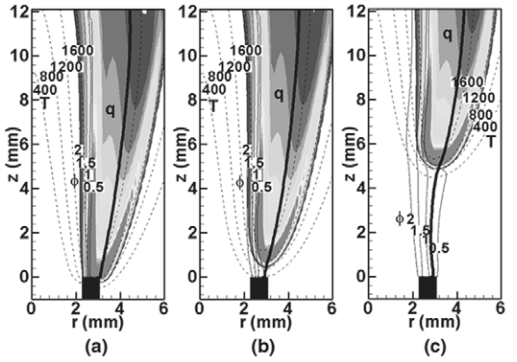

FIG. 5. Simulated isotherms, equivalence ratio, and heat release rate contours (that begin at 50 J/(cm^3 s) with a 100 J/(cm^3 s) interval) at three different times: (a) attached flame, $t = 0$; (b) lifted flame, $t = 20$ ms; (c) lifted flame, $t = 100$ ms. The thick solid line represents the stoichiometric mixture fraction $\xi_{st} = 0.383$.

frame of reference, $\hat{n}$ is the normal to the flame surface defined as $\hat{n} = -\nabla\varphi/|\nabla\varphi|$, $\nabla \cdot \hat{n}$ is the curvature of the flame front, and the subscript t denotes the tangential component of the velocity. After algebraic manipulation, we can express flame stretch as

$$\kappa = \nabla \cdot V_{fluid} - \hat{n}\hat{n}: \nabla V_{fluid} + S_d(\nabla \cdot \hat{n}). \quad (4)$$

In the relation above, the first two terms represent the effect of a non-uniform tangential flow field along the flame surface and we use the term hydrodynamic stretch κ_h to represent them. The last term in equation 4 represents the effect due to the unsteady propagation of a curved flame surface and is the curvature-induced stretch κ_c. It is useful to address the effects of these two kinds of stretch on the triple flame propagation speed.

Flame-Lifting Process

Figure 5 presents the computed flame structure at the base of a triple flame at three different times during the process of liftoff from the burner wall for case T2. For each image, the heat release rate, temperature, and equivalence ratio contours are plotted. The thick solid line corresponds to stoichiometric mixture fraction contour. Adiabatic boundary condition was imposed on the burner wall in Fig. 5a so that the wall serves as a flame holder. At the boundary where wall and flame are adjacent, the wall temperature can be as high as 1600 K, which is not realistic when compared with experiments. The ξ_{st} contour begins at the outer edge of the burner wall and passes through the center of the flame. On the contrary, the $\phi = 1$ contour is located on the rich side of the flame and suggests that for rich partially premixed flames the stoichiometric contour of mixture fraction is more useful than that of equivalence ratio. In Fig. 5b and c, the wall boundary is changed to isothermal (at 294 K) and the unsteady flame liftoff phenomenon is depicted. The flame moves downstream along the ξ_{st} contour, which is a characteristic property of triple flames. After ≈100 ms the flame stabilizes at a position $z = 4.92$ mm, which is slightly lower than the experimentally obtained value of 5.5 mm. There is a low axial velocity region behind the burner rim that stabilizes the flame and is dominated by diffusion. The base of the triple flame becomes more rounded and wider and moves away from the centerline with an increase in the liftoff height.

In Table 1, we provide the values of some relevant properties of the triple point at four different times during flame liftoff for case T2, along with two stable states for cases T1 and T3. When the flame moves downstream, the curvature decreases (as is observed from C_2* images in Fig. 1) because of the flow dilatation ahead of the triple point. Table 1 shows that

TABLE 1
Flame characteristics at the triple point during flame liftoff for three cases corresponding to Fig. 4[a]

Case	Time (ms)	r (mm)	z (mm)	V_{in} (m/s)	Curvature $\nabla \cdot \hat{n}$ (mm^{-1})	κ_h (s^{-1})	κ_c (s^{-1})	κ (s^{-1})	S_d (m/s)	V_a (m/s)
	20	2.91	2.75	0.6	849.1	−100.3	260.0	159.7	0.31	0.38
T2	40	3.04	3.66	0.6	678.2	−35.2	232.7	197.5	0.35	0.37
	60	3.10	4.22	0.6	617.7	6.7	240.6	247.3	0.38	0.38
	100	3.17	4.92	0.6	577.2	39.3	228.1	267.4	0.39	0.39
T1	200	3.07	3.80	0.4	653.9	4.6	254.5	259.1	0.38	0.37
T3	200	3.30	8.00	0.8	498.1	86.5	224.0	310.5	0.45	0.43

[a]For case T2, the flame characteristics during temporal evolution of the triple flame as it lifts off from the burner and then stabilizes at some downstream location are provided at four different times. For cases T1 and T3, the flame characteristics correspond to the final stabilized state.

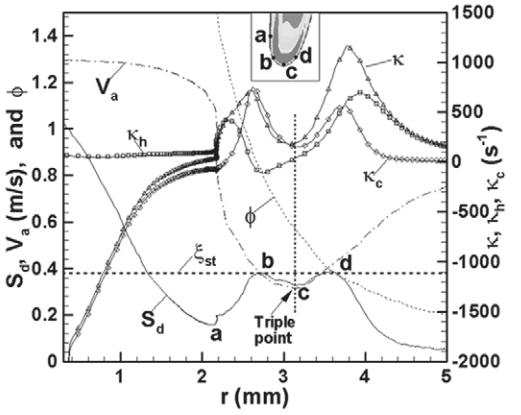

FIG. 6. Simulated flame propagation speed S_d, axial velocity V_a, equivalence ratio ϕ, and stretch rate (κ, κ_h, and κ_c) along the flame front for case T2. The dashed thick line represents the stoichiometric mixture fraction and the vertical dotted line represents the triple point location. The inserted small figure indicates the locations of points *a* to *d*.

S_d is smaller than the axial flow velocity V_a at the initiation of liftoff. κ_h increases from a negative to a positive value, and κ_c slightly decreases. The overall stretch is positive and increases as the flame lifts. S_d gradually increases and becomes equal to V_a that is almost constant during the flame liftoff phenomena.

The curvature of a premixed flame influences the upstream transport of both heat and flame radicals [20]. When a flame surface is convex toward the upstream flow, heat is defocused away from the flame and flame radicals are focused toward the flame. For a rich methane-air flame with a large convex curvature, such as at the base of a triple flame, the decrease in flame speed by κ_c surpasses the decrease in the flow velocity that is manifest through streamline divergence. Consequently, this results in a lower S_d so that such a flame is more readily lifted. Since the local equivalence ratio near the triple point is lower than unity (as can be seen from Fig. 5), the effective Lewis number (*Le*) of the mixture is also less than unity, and the flame propagation speed increases with the increasing stretch that is experienced at higher liftoff heights [20]. The flame becomes more inclined toward the centerline as it lifts off (cf. Fig. 5c). This has the effect of increasing S_d, since now only the normal component of the flow velocity to the flame surface must be balanced against the burning velocity. The lifted flame stabilizes because of the combined effects of flame stretch, flow redirection, and flame inclination, and the flame propagation speed assumes a value that is roughly equivalent to the velocity normal to the flame front at the triple point.

Comparing the properties at the stable state of cases T1, T2, and T3, it is seen that, in a manner similar to our experimental results, the liftoff height increases linearly with respect to V_{in}, and the flame base moves further away from the centerline. The values of the curvature and χ_{st} decrease, while those of κ, S_d, and V_a increase.

Stretch Effects on Lifted Flames

Figure 6 presents the flame propagation speed, axial velocity, equivalence ratio, and stretch rate along the flame front (i.e., the OH mass fraction contour of 2.0×10^{-5}) for case T2. The dashed thick line represents ξ_{st}, and the vertical dotted line represents the triple point location. V_a exhibits a minimum at the triple point and a maximum at the flame tip. S_d also has a maximum value at the flame tip and monotonically decreases along the flame surface until a turning point *a* where κ changes sign from negative to positive. It then exhibits two peaks at the point *b* and *d*, and a relatively low value at point *c* (which is the triple point). The variation of κ follows a similar behavior, and demonstrates a good correlation between κ and S_d. For instance, from the flame tip to point *a*, S_d is higher than the unstretched flame speed value and decreases as the stretch increases.

At turning point *a* the hydrodynamic stretch κ_h and curvature stretch κ_c have similar absolute values but have opposite signs so that their sum $\kappa \approx 0$. This results in an unstretched flame speed of 16 cm/s, which is virtually identical to the laminar burning velocity for a stoichiometric methane-air mixture diluted with 25% nitrogen. The value of κ_c reaches a maximum positive value of 695 s^{-1} approaching point *b*, while κ_h is near zero (-28 s^{-1}). In the region from *a* to *b*, *Le* is slightly larger than unity, and the flame experiences positive stretch. In this region, S_d increases with increasing positive stretch although $Le > 1$. This behavior appears to be anomalous in the context of the theoretical correlation among S_d, κ_h, and *Le* [20]. However, the region is characterized by strong interactions between the rich premixed and non-premixed reaction zones, and may not be amenable to simple interpretation. In the region extending from points *c* through *d* into the lean region, since $\phi < 1$ and $Le < 1$, S_d increases (decreases) with increasing (decreasing) positive stretch rate.

Near the flame tip, the flame is subjected to large negative stretch and $|\kappa_h| \ll |\kappa_c|$. S_d is two times larger than the stoichiometric laminar burning velocity, and linearly decreases with an increase in κ, which is consistent with the theoretical correlation. On the contrary, at the flame base, that is, near the triple point, the flame experiences small positive stretch and S_d attains a relatively constant value. However, in the lean premixed region following the triple point (where $Le < 1.0$), S_d increases (decreases) with an increase (decrease) in κ. This is consistent with the

theoretical correlation discussed by Law and Sung [20] in the context of simple premixed flames.

Conclusions

The liftoff height of triple flames established in the near field of the burner increases linearly with the inner-flow velocity V_{in} at relatively low values. As V_{in} exceeds a critical velocity, the flame becomes unstable and oscillates, with blowout occurring occasionally after some periodic displacements. At even higher velocities, the flame directly blows out. Two kinds of instabilities are observed. One has a uniform frequency of $\approx$16 Hz for various V_{in} values, and the corresponding flames are relatively stable at their base. These oscillations are assumed to occur because of flow instabilities. The other kind of instability has a lower frequency but larger amplitude, and is surmised to be due to buoyancy effects.

At the flame base, that is, at the triple point, the overall stretch rate is positive and increases as the flame lifts, while the curvature decreases. The flame propagation speed gradually increases during the unsteady liftoff phenomena and becomes equal to the axial flow velocity (which remains virtually unchanged). The flame lifts off to a location at which the combined effects of flame stretch and flow redirection favor its stability. The flame becomes more inclined toward the centerline as it lifts off, which increases the flame propagation speed. There is a good correlation between the stretch rate, Lewis number, and flame propagation speed in both the rich and lean premixed zones of the lifted triple flame. However, near the triple point, which is characterized by strong interactions among the three reaction zones, the correlation becomes significantly more complex.

Acknowledgments

This research was supported by the National Science Foundation Combustion and Plasma Systems Program for which Dr. Farley Fisher is the Program Director, and by the NASA Microgravity Research Division for which Dr. Uday Hegde serves as the technical monitor. Many fruitful discussions with Dr. V. R. Katta of ISSI are greatly appreciated.

REFERENCES

1. Vervisch, L., *Proc. Combust. Inst.* 28:11 (2000).
2. Chung, S. H., and Lee, B. J., *Combust. Flame* 86:62 (1991).
3. Lee, B. J., and Chung, S. H., *Combust. Flame* 109:163 (1997).
4. Kioni, P. N., Rogg, B., Bray, K. N. C., and Liñán, A., *Combust. Flame* 95:276 (1993).
5. Ghosal, S., and Vervisch, L., *Combust. Flame* 123:646 (2001).
6. Liñán, A., in *Combustion in High Speed Flows* (J. Buckmaster, T. L. Jackson, and A. Kumar, eds.), Kluwer Academic, Boston, 1994, p. 461.
7. Takahashi, F., Schmoll, W. J., and Katta, V. R., *Proc. Combust. Inst.* 27:675 (1998).
8. Shu, Z., Krass, B. J., Choi, C. W., Aggarwal, S. K., Katta, V. R., and Puri, I. K., *Proc. Combust. Inst.* 27:625 (1998).
9. Ratti, S., "An Experimental Study on the Structure of Triple Flames Stabilized on a Slot Burner," M.S. thesis, University of Illinois at Chicago, 1999.
10. Katta, V. R., Goss, L. P., and Roquemore, W. M., *Combust. Flame* 96:60 (1994).
11. Shu, Z., Aggarwal, S. K., Katta, V. R., and Puri, I. K., *Combust. Flame* 111:276 (1997).
12. Peters, N., "Reduced Kinetic Mechanisms for Applications in Combustion Systems," in *Lecture Notes in Physics, Vol. m15* (N. Peters and B. Rogg, eds.), Springer-Verlag, New York, 1993.
13. Xue, H., and Aggarwal, S. K., *AIAA J.* 39(4):637 (2001).
14. Won, S. H., Chung, S. H., Cha, M. S., and Lee, B. J., *Proc. Combust. Inst.* 28:2093 (2000).
15. Bilger, R. W., *Proc. Combust. Inst.* 22:475 (1988).
16. Najm, H. N., and Wyckoff, P. S., *Combust. Flame* 110:92 (1997).
17. Im, H. G., and Chen, J. H., *Combust. Flame* 119:436 (1999).
18. Jhalani, A., Mukhopadhyay, A., and Puri, I. K., "An Investigation of Stretch Effects on Rich Premixed Burner-Stabilized Flames," paper 01F-3, Western States Section Fall Meeting of the Combustion Institute, Salt Lake City, 2001.
19. Chung, S. H., and Law, C. K., *Combust. Flame* 55:123 (1984).
20. Law, C. K., and Sung, C. J., *Prog. Energy Combust. Sci.* 26:459 (2000).

COMMENTS

Joel Daou, UMIST, UK. The relation between local burning speed and stretch has been derived for the case of homogeneous mixtures (i.e., without concentration fluctuations). Could you comment on or justify the use of such relations in the case of triple flames?

Author's Reply. We are not sure what relation between local burning speed and stretch you are referring to. If you are referring to the linear relationship as reported by Law and Sun (Ref. [20] in paper), we did not use that relationship. Since both the local burning speed and stretch are

local properties and are defined using fundamental equations (Ref. [18] in the paper), they do not require any assumption such as homogeneous mixtures.

•

James F. Driscoll, University of Michigan, USA. The displacement speed that you report is an important quantity, but it has been defined in different ways by different authors. Did you determine it by using local gas velocity and local scalar properties along an isoline near the leading edge or the trailing edge of the flame, and is stretch the reason why it exceeds the unstretched laminar burning velocity? The stretch rate is made up of two components: one due to strain and one due to curvature; please comment on which of these two components is larger in your case.

Author's Reply. As described in the paper, the displacement speed is defined by using local gas velocity and local scalar properties along an OH isocontour at the leading edge. Stretch is the main reason that local displacement speed exceeds the unstretched laminar burning velocity, but the local displacement speed can also be affected by other factors, such as Lewis number, and so forth. In Fig. 6, we show the stretch rate (overall stretch rate κ, hydrodynamic stretch κ_h, and curvature stretch κ_c) along the flame front. It can be seen that at the tip of the flame, curvature stretch κ_c is dominant and has a large negative value. When approaching the triple point, κ_c increases to positive values and is of the same order as κ_h.